Angewandte Chemie
Eine Zeitschrift der Gesellschaft Deutscher Chemiker

Supporting Information

69451 Weinheim, Germany

Probing Secondary Structures of Spin-Labeled RNA by Pulsed EPR Spectroscopy**

Giuseppe Sicoli, Falk Wachowius, Marina Bennati, and Claudia Höbartner**

anie_201000713_sm_miscellaneous_information.pdf

Table of Contents

RNA solid-phase synthesis, deprotection and purification

5'-*O*-DMT-2'-*O*-TOM- protected nucleoside 3'-β-cyanoethyl phosphoramidites of N^6-acetyladenosine, N^4-acetylcytidine, N^2-acetylguanosine and uridine were obtained from ChemGenes, Wilmington, USA. O^6-(4-chlorophenyl)-5'-*O*-DMT-2'-*O*-tBDMS-inosine 3'-β-cyanoethyl phosphoramidite, 2-fluoro-5'-*O*-DMT-O^6-(4-nitrophenyl)-2'-*O*-tBDMS-inosine 3'-β-cyanoethyl phosphoramidite, and O^4-(4-chlorophenyl)-5'-*O*-DMT-2'-*O*-tBDMS-uridine 3'-β-cyanoethyl phosphoramidite were obtained from Berry&Associates, Ann Arbor, USA.

All oligoribonucleotides were synthesized on polystyrene custom primer supports from GE Healthcare on a Pharmacia Gene Assembler Plus or on an ÄKTA Oligopilot 10 Plus, following slightly modified DNA standard methods. Detritylation was achieved with dichloroacetic acid/1,2-dichloroethane (3:97, v/v) for two minutes. For coupling, 75 µl of 0.1 M phosphoramidites in acetonitrile was activated by 250 µl of 0.25 M benzyl thiotetrazole in acetonitrile; coupling time for TOM amidites was 4 min, coupling time for tBDMS-protected amidites was 12 min. Capping was achieved with 1:1 (v/v) A/B for one minute (A, Ac_2O/sym-collidine/acetonitrile, 2:3:5, by vol.; B, 0.5 M 4-(dimethylamino)pyridine in acetonitrile). Oxidation was done with 10 mM I_2 in acetonitrile/sym-collidine/water (10:1:5, by vol.) for one minute. Amidite solutions, tetrazole solutions, and acetonitrile were dried over activated molecular sieves overnight. All sequences were synthesized trityl-off on 0.7-1.0 µmol custom primer support.

Deprotection and cleavage of unmodified RNA oligonucleotides from solid support were achieved with $MeNH_2$ in EtOH (8 M, 500 µL) and $MeNH_2$ in water (40%, 500 µL) for six hours at 37°C; the solution was then evaporated to dryness. Removal of the 2'-*O*-silyl groups was afforded by treatment with tetrabutylammonium fluoride trihydrate (TBAF·$3H_2O$) in THF (1 M, 500 µL) for at least 12 hours at room temperature. The reaction was quenched by the addition of Tris.HCl (1 M, pH 7.4, 500 µL). The volume of the solution was reduced to 0.5 ml and directly applied on a Sephadex G 10 column (3x5 ml HiTrap columns, GE Healthcare) monitored by UV-detection at 280 nm. The product was eluted with water and evaporated to dryness.

RNA oligonucleotides were purified by anion-exchange chromatography or by denaturing polyacrylamide gel electrophoresis (PAGE). Anion exchange HPLC was performed on a semipreparative Dionex DNAPac column at 80 °C. Flow rate: 2 ml/min: eluant A, 25 mM Tris.HCl, 6 M urea, in water (pH 8.0); eluant B, 25 mM Tris.HCl, 0.5 M $NaOCl_4$, 6 M urea, (pH 8.0); detection at 265 nm; gradient I (for checking the purity of crude products after deprotection): 45 minutes 0–60% B in A; gradient II (for purification): 10–15% B in A within 30 minutes. Fractions containing the purified oligonucleotide were desalted by loading onto a C18 SepPak cartridge (Waters/Millipore), followed by elution with 100 mM NaCl, water, and then water/CH_3CN (6:4, v/v). Combined fractions containing the oligonucleotide were lyophilized to dryness.

PAGE purification was performed on 15% or 20% denaturing acrylamide gels containing 7 M urea; gels were 0.7 or 1.5 mm thick, 20 x 30 cm, 2 or 4 lanes, running buffer 1x TBE (89 mM each Tris and boric

acid, pH 8.3, 2 mM EDTA), at 35 W. RNA was visualized by UV shadowing and extracted by crush and soak into TEN (10 mM Tris.HCl, pH 8.0, 1 mM EDTA, 300 mM NaCl) at 37°C for 2x 3-5h, followed by precipitation with ethanol at -80°C.

Synthesis of TEMPO-labeled RNA

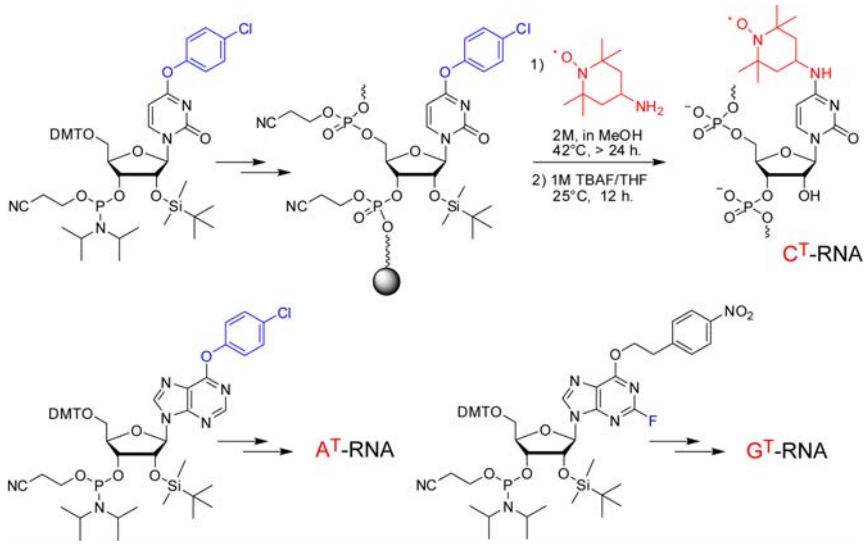

RNA oligonucleotides containing the convertible nucleotides were assembled on solid-phase as described above. The nitroxide reagent 4-amino-2,2,6,6-tetramethylpiperidin-1-oxyl, (50 mg, 0.3 mmol) was dissolved in methanol (120 µL), and the polystyrene support containing the modified RNA (ca 5 mg PS support, containing ca 0.4 µmol RNA) was added. The tube was tightly sealed with parafilm and incubated at 42 °C for at least 24 hours (up to 96 hours for TEMPO-A; or 48 h at 55°C). The support was occasionally suspended by brief vortexing. The support was pelleted by centrifugation, and the orange-colored supernatant was transferred into a 10 mL round-bottom flask. The support was washed twice with 200 µL methanol, and twice with 500 µL 50% aq. ethanol (the remaining support was then colorless). The combined solutions were evaporated under reduced pressure at 50°C. The residue was dissolved in 500 µL of 1 M TBAF in THF, and the orange solution was incubated at 25-30°C for 12 hours. After the addition of 500 µL of 1 M Tris.HCl, pH 8.0, the solution was concentrated to 500 µL to remove THF. The crude TEMPO-RNA was isolated by size-exclusion chromatography on Sephadex G10 by elution with water. The crude product was analyzed by anion exchange HPLC on a Dionex DNAPac PA 200 column, and then purified by denaturing PAGE (20% acrylamide, 7 M urea) or by denaturing anion exchange HPLC in the presence of 6 M urea, at 80°C. Ethanol precipitation or SepPak desalting were performed under standard conditions.

Figures S1 and S2 depict examples of anion exchange HPLC traces of crude and purified double TEMPO-labeled RNA oligonucleotides. The substitutions of 4-ClPh-U to C^T and of 2-F-I to G^T occurred smoothly and yielded one major product which could easily be purified. In contrast, the substitution of 6-ClPh-I to A^T was slow and yielded a mixture of products that were separable by anion exchange HPLC. The three major products were isolated and characterized by MS. Besides incomplete substitution (byproduct b), a partially hydrolyzed product was observed that contained only one TEMPO group (byproduct a).

Figure S3 depicts analysis and purification of TEMPO-labeled human telomeric repeat RNA **11**. The substitution of 6-ClPh-I was not complete after 96 h at 42°C, but the desired product could be easily separated by PAGE. The isolated products were analyzed by anion exchange HPLC. The unsubstituted byproduct (a) was identified as the 4-ClPh-containing RNA by MS analysis.

The isolated yields of TEMPO-labeled RNA ranged from 20-100 nmol.

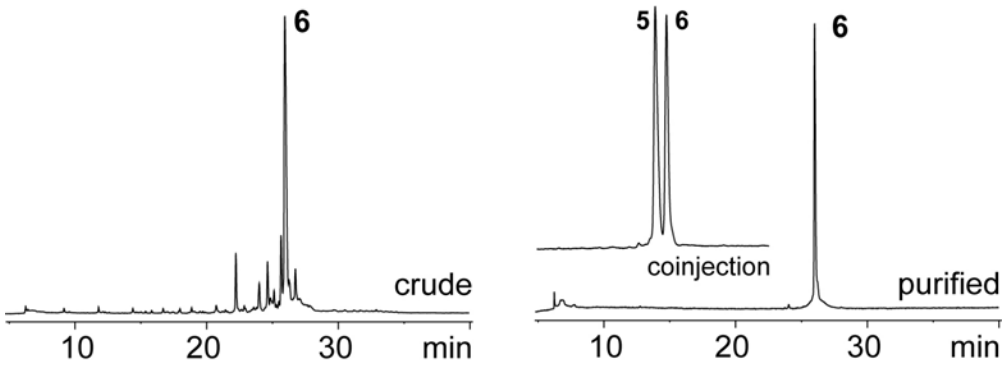

Figure S1. Anion exchange HPLC analysis of crude and purified C^T-containing 13 nt long RNA **6**. The inset shows the coinjection of **6** with the analogous unmodified RNA **5**.

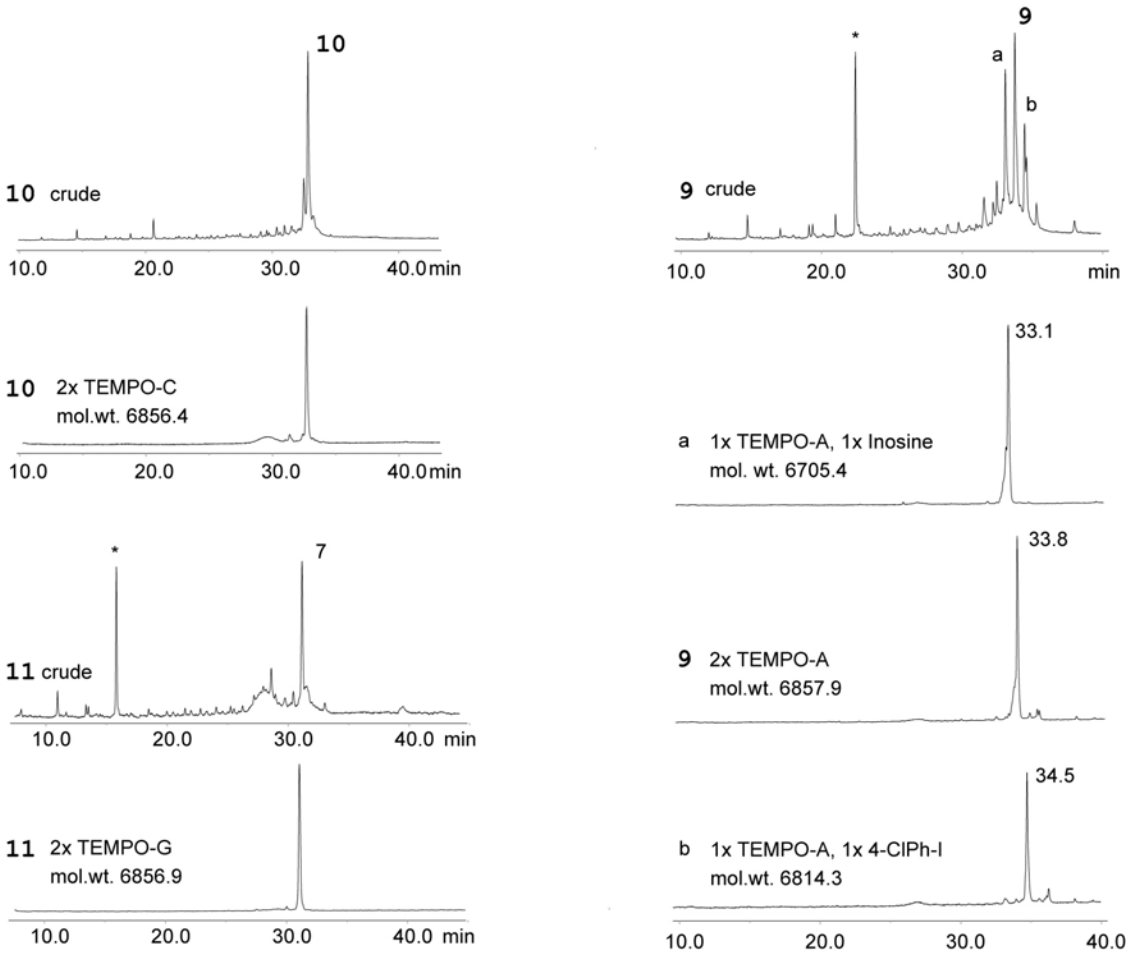

Figure S2. Examples of anion exchange HPLC traces of crude and purified TEMPO-labeled RNA oligonucleotides (see Table S1 for sequence information). The asterisk denotes abort products from incomplete coupling of the 2'-*O*-TBDMS-protected convertible nucleoside phosphoramidites.

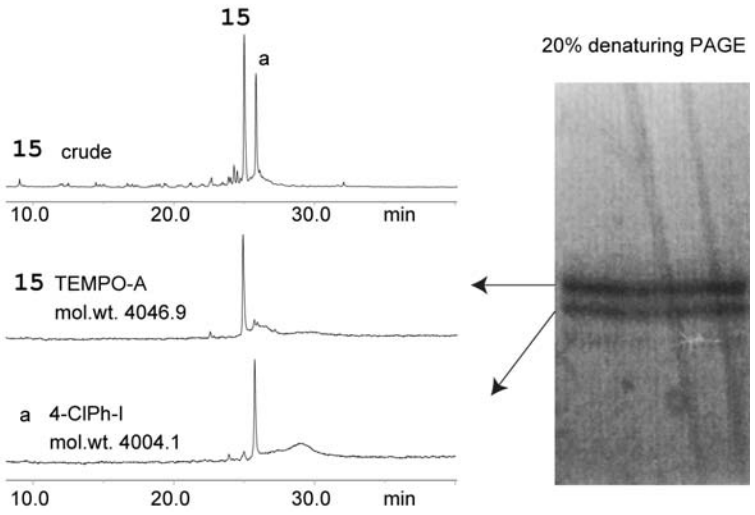

Figure S3. Analysis and purification of A^T-labeled RNA **15** UAGGGUU**A^T**GGGU.

MS analysis

The masses of the isolated RNA oligonucleotides were confirmed by MALDI-TOF or ESI mass spectrometry in the bioanalytical mass spectrometry group of Dr. Henning Urlaub at MPIbpc.

Table S1. MS characterization of RNA oligonucleotides

No	5'-Sequence-3'	$M_{calcd.}$ [amu]	$M_{obs.}$ [amu][a]
5	CGCGAACGCGA	4139.6	4139.7 [E]
6	CG**C^T**GAACGCGA	4293.8	4293.9 [E]
7	GACGUCGGAAGACGUCAGUA	6549.0	6549.0 [E]
8	UACUGACGUCUUCCGACGUC	6279.8	6280.2 [E]
9	G**A^T**CGUCGGAAG**A^T**CGUCAGUA	6857.4	6857.9 [M]
10	GA**C^T**GUCGGAAGA**C^T**GUCAGUA	6857.4	6856.4 [M]
11	GAC**G^T**UCGGAAGAC**G^T**UCAGUA	6857.4	6856.9 [M]
12	GACGU**C^T**GGAAGACGU**C^T**AGUA	6857.4	6859.8 [M]
13	GACGU**C^T**GGAAGACGUCAGUA	6703.2	6705.7 [M]
14	UAGGGUUAGGGU	3892.4	3893.1 [E]
15	UAGGGUU**A^T**GGGU	4046.6	4046.9 [E]

[a] E = ESI, M = MALDI.

Estimation of distances between spin labels

Models of A-from RNA duplexes were built via the *make-na* server:

http://structure.usc.edu/make-na/server.html.

The estimated distances reflect the distances between the nitrogen-atoms to which the TEMPO groups are attached.

Table S2. Estimated and experimental distances between TEMPO-labels in RNA duplexes.

No	duplex 5′-RNA-3′ 3′-RNA-5′	Estimated distance (between attachment sites in a standard A form duplex) [nm]	Measured distance by PELDOR [nm] (between two TEMPO groups)
6	CG**C^T**GAAUUCG CGA AGCG CUUAAG**C^T**GC	1.9	2.0 ± 0.2
9/7	G**A^T**CGUCGGAAG**A^T**CGUCAGUA CU GCAGCCUUCUG CAGUCAU	2.8	3.1 ± 0.2
10/7	GA**C^T**GUCGGAAGA**C^T**GUCAGUA CU GCAGCCUUCUG CAGUCAU	2.8	3.1 ± 0.2
11/7	GAC**G^T**UCGGAAGAC**G^T**UCAGUA CU GCAGCCUUCUG CAGUCAU	2.8	3.2 ± 0.3
12/7	GACGU**C^T**GGAAGACGU**C^T**AGUA CU GCAGCCUUCUG CAGUCAU	2.8	3.1 ± 0.2

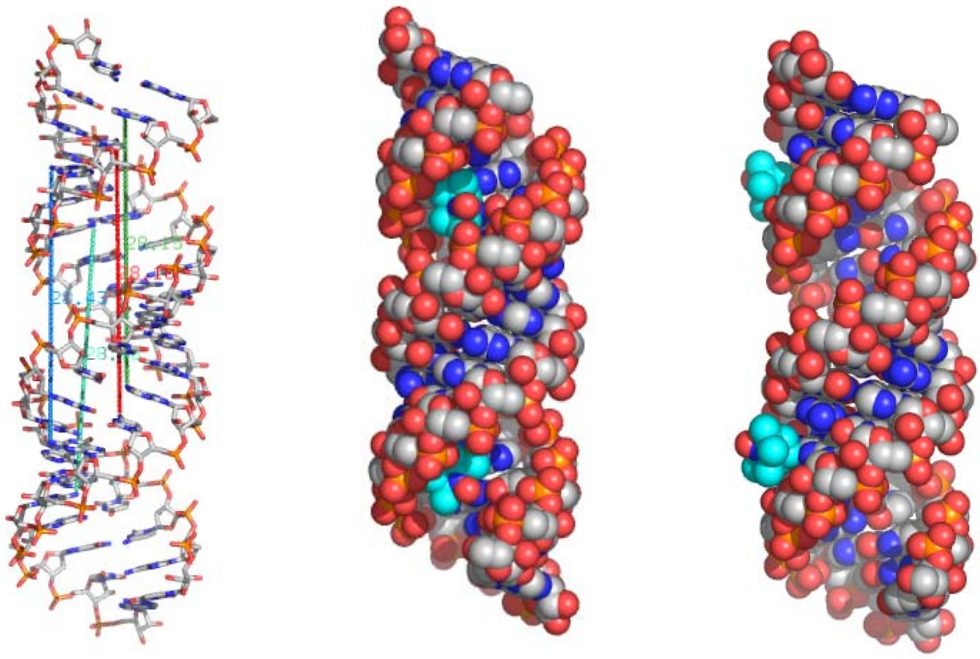

Figure S4. Structural context of TEMPO-labeled RNAs. Left: **8**/7 with distances marked between N6 of A2/12 (green), N4 of C3/13 (red) and C6/16 (cyan), and N2 of G4/14 (blue, numbers are in Å). Middle: space-filling model of **12**/**7** showing TEMPO groups on C6 and C16 burried in the major groove. Right: space-filling model of **11**/**7** with TEMPO groups on G4 and G14 in the minor groove. Carbon atoms of TEMPO groups are in cyan. Images were rendered in Pymol using pdb files generated by the *make-na* server, hydrogen atoms are not shown (TEMPO groups were built in Pymol, no energy minimization was performed on these models).

EPR Spectroscopy

Sample preparation

Nitroxide-labeled RNA oligonucleotides **9-13** were individually mixed with 1.5 equivalents of unlabeled complementary RNA **7** in 10 mM K_2HPO_4 buffer, pH 7.0, containing 150 mM NaCl. The solution was heated to 90°C for 3 min and slowly cooled to 25°C. Before insertion into the resonator, 15% glycerol was added as a cryoprotectant to a final RNA concentration of 20 to 60 µM in a sample volume of 65 µL, followed by flash freezing using liquid nitrogen. For the titration experiment of Figure 5, the unlabelled RNA **7** was added in four separate steps from a 500µM stock solution to RNA **12** at a concentration of 30 µM, followed by denaturation and annealing after each addition (the concentration of **12** changed by less than 10% over all titration steps).

Continuous wave EPR spectroscopy measurements

EPR spectra were obtained using 10 µL of sample placed in glass capillaries (1.0 × 1.2 mm) sealed at one end. X-band EPR spectra were acquired on a Bruker EleXsys Spectrometer using an ELEXSYS super high sensitivity probehead. The incident microwave power was 2 mW, the field modulation was 1.0 or 1.5

G at a 100 kHz frequency. Sample temperatures were set at 25 °C. For each sample, 60 – 100 scans were collected and averaged.

Pulsed EPR spectroscopy measurements

Double Electron-Electron Resonance (DEER) measurements were performed using a Bruker EleXsys 580 spectrometer equipped with a dielectric resonator at a temperature of 40 K. The four-pulse DEER sequence $(\pi/2)_{\nu 1}$–τ_1–$(\pi)_{\nu 1}$–τ–$(\pi)_{\nu 2}$– τ_1 + τ_2–τ–$(\pi)_{\nu 1}$–τ_2–echo was used in each of the RNA distance determinations; the ELDOR pulse (ν_2, 12 ns or 32 ns) was positioned at the centerfield maxima of the echo-detected nitroxide spectrum, whereas the $\pi/2$ and π observe pulses (ν_1, 16 and 32 ns) were positioned at the low field line of the spectrum ($\nu_1 - \nu_2 \approx 75$ MHz). A model-free analysis of DEER data was performed by applying Tikhonov regularization, using the *L* curve as criterion for optimal parameter regularization. Primary experimental data were background-corrected by fitting an decay function *B*(*t*) for the intermolecular contribution, followed by normalization of the function. The form factor *F*(*t*) obtained in this way was then processed by Tikhonov regularization. All model-free processing was performed with the program DeerAnalysis 2008.[1]

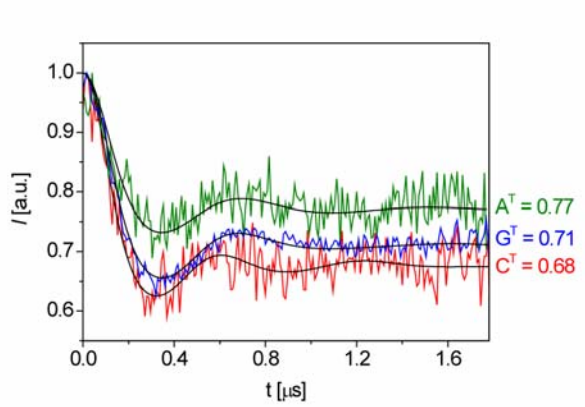

Figure S5. Dipolar evolution functions for the duplexes **9**/**7** (green), **10**/**7** (red) and **11**/**7** (blue) using a strong inversion pulse of 12 ns (10-20 scans). The observed modulation depths are consistent with those reported for other double-labeled RNA systems.

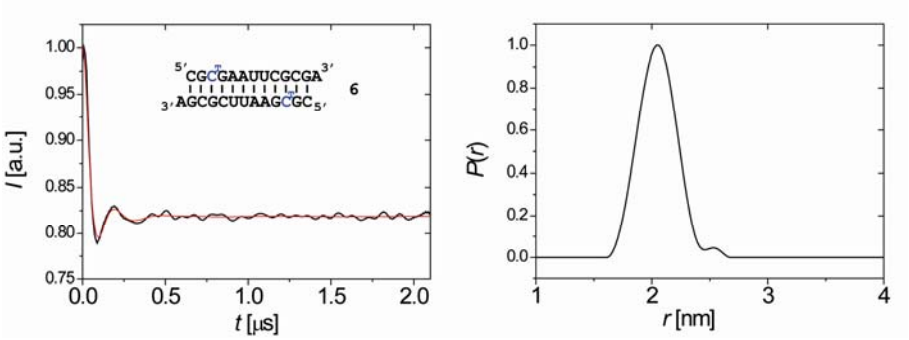

Figure S6. PELDOR of RNA **6**; *left*: dipolar evolution function, *right*: distance distribution.

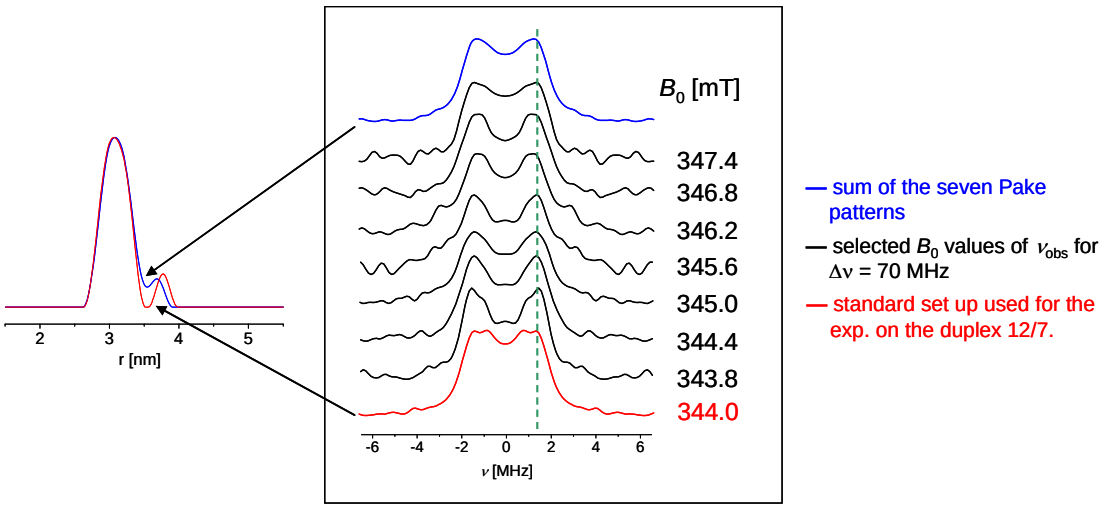

Figure S7. Orientation averaging experiment (blue line) and standard PELDOR set up on the duplex **12**/**7** (red line).

UV melting curves

For duplex and hairpin secondary structures, absorbance versus temperature profiles were recorded at 250 nm, 260 nm, 265 nm, and 270 nm on a Cary-100 spectrophotometer equipped with a multiple cell holder and a Peltier temperature-control device. Samples contained 1 to 30 µM RNA in buffer solutions of 10 mM K_2HPO_4 and 150 mM NaCl at pH 7.0. A layer of silicon oil was placed on the surface of the solution to prevent evaporation during the experiment. Data were collected every 0.2 or 0.5°C after a complete cooling and heating cycle (3°C to 95°C) at a heating/cooling rate of 0.7 °C/minute. Melting transitions were reversible for all RNAs and essentially the same with respect to the four different wavelengths. Melting curves for unmodified and spin-labled hairpin and duplex RNAs are depicted in Figures S8 and S9. Thermodynamic parameters for RNAs **5** and **6** were obtained from concentration-dependent melting curves by analysis of $\ln(c_T)$ vs $1/T_m$ (Figure S8).

For quadruplex RNAs, absorbance versus temperature profiles were recorded at 245 nm, 250 nm, 260 nm, 280 nm, 295 nm, and 320 nm. Clear hyperchromicity profiles were observed at 245 and 280 nm, and the characteristic hypochromic melting curve was obtained at 295 nm. Melting curves of quadruplex RNAs **14** and **15** were measured at a concentration of 7 µM RNA in 20 mM K_2HPO_4, 70 mM KCl, pH 7.0. The heating /cooling rate was 0.2 °C/min. Experiments done at 0.7°C/min lead to more pronounced hysteresis effects(Figure S10).

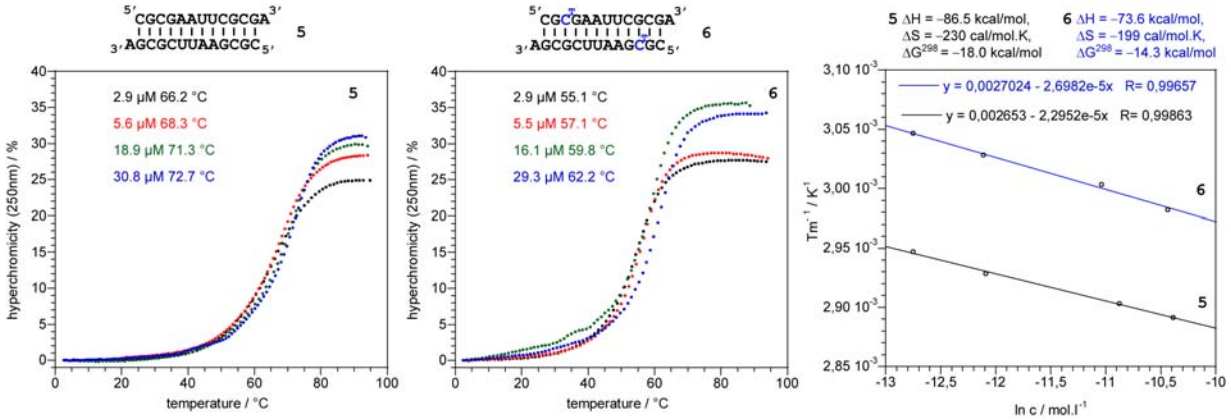

Figure S8. UV melting analysis of RNAs **5** and **6** at four different concentrations.

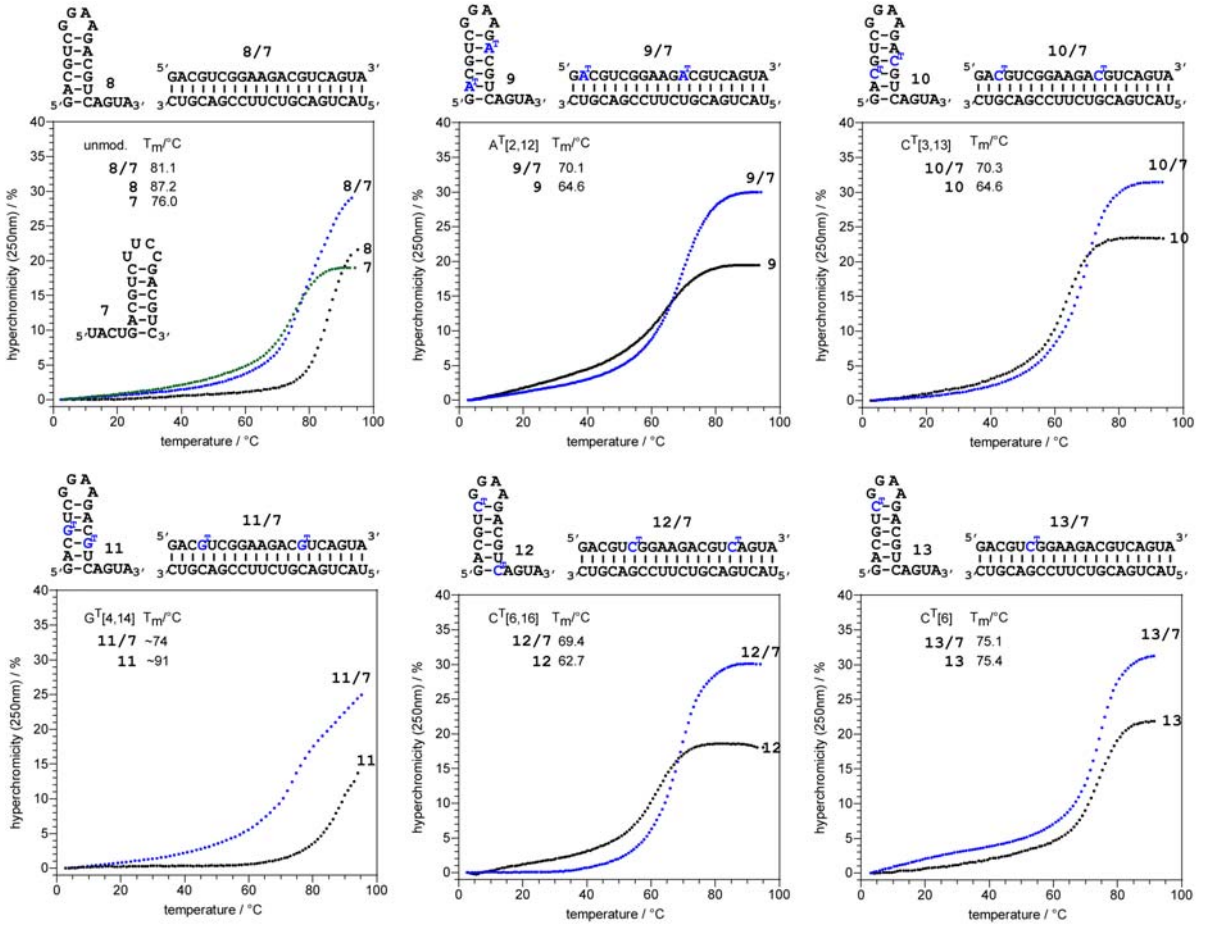

Figure S9. UV melting curves of unmodified and spin-labeled hairpin and duplex RNAs **7**-**13** (2 µM. strand conc.).

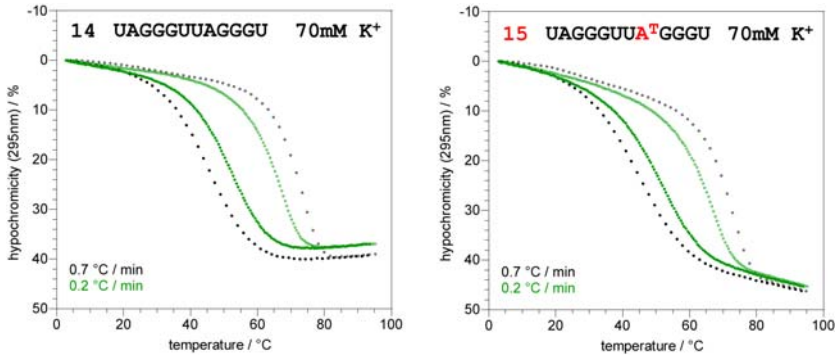

Figure S10. Melting curves of quadruplex RNAs at different heating and cooling rates.

G-quadruplex structures

The pdb files of the published RNA quadruplex structure was used to estimate the expected distance between two TEMPO groups by measuring the distance between the attachment sites, i.e., the N^6 atoms of adenosine A8 (A8 and A20 in the pdb file 1KBP [ref 17 in manuscript]). This distance is 3.7 nm and compares well with the distance obtained by PELDOR experiments (Figure 3 in manuscript). The conserved folding topology for human telomeric RNA quadruplexes[2] makes the estimation of the distance between the TEMPO groups in an antiparallel RNA quadruplex structure rather difficult. Therefore we chose to compare the RNA structure with several reported DNA quadruplex structures of human telomeric repeat sequences (Figure S11). The X-ray crystal structure of the 12 nt DNA sequence analogous to RNA **14** was reported in 2002.[3] The distance of 3.5 nm between the N^6 attachment sites on A8 and A20 in PDB file 1K8P[3] compares very well with the distance of 3.7 nm in the RNA structure. Similarly, in an analogous monomolecular parallel-stranded G-quadruplex of a 22 nt DNA (pdb 1KF1[3]), the distance between the N^6 atoms of analogous positions A7 and A19 is 3.4 nm. In sharp contrast, the two adenosines come in close proximity in an antiparallel basket-type G-quadruplex structure of the same 22 nt DNA sequence. The distance between the N^6 atoms of A7 and A19 is less than 1 nm according to pdb 143D[4]. In a different DNA topology, the (3+1) hybrid DNA quadruplex structure (pdb 2GKU[5], the two N^6 atoms of the corresponding adenosines at position 8 and 20 are 1.9 nm apart. From this comparison of different DNA quadruplex topologies we conclude that the distance between the TEMPO groups in RNA **15** would likely need to be less than 2 nm, if this RNA could fold into an antiparallel quadruplex structure (which is unlikely). Such a short distance was not observed in our PELDOR experiment, which is consistent with the reported conserved parallel topology, which is also supported by the CD spectroscopy results. (Briefly, parallel quadruplex conformations show a maximum at 260 nm, and a minimum at 240 nm, whereas antiparallel DNA quadruplex conformations generally show a maximum CD effect at 290-295 nm, and a minimum around 260 nm).

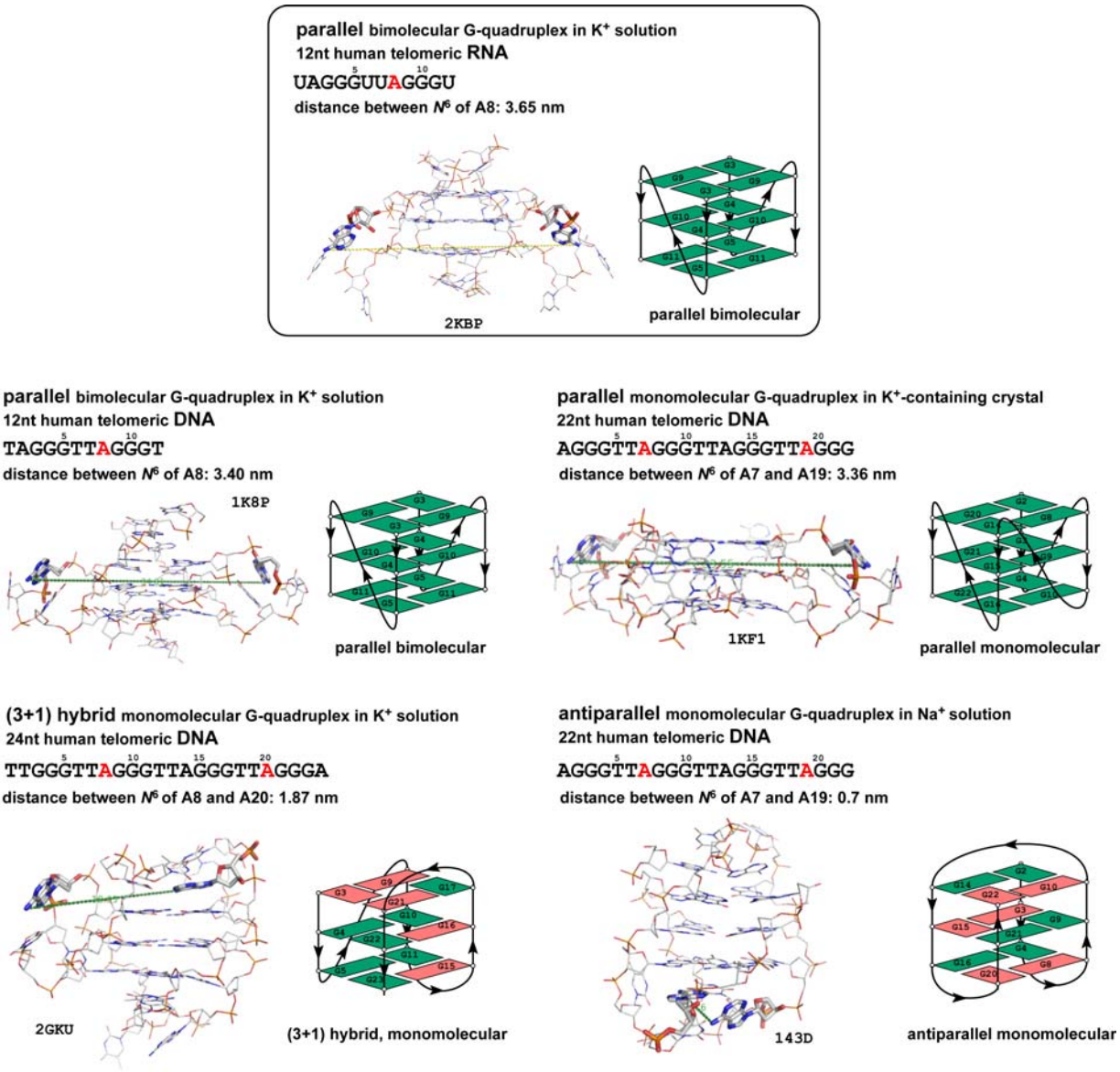

Figure S11. Overview of different quadruplex folding topologies reported for RNA and DNA human telomeric repeats. The adenosines corresponding to the positions that carry the TEMPO label in our RNA quadruplex construct are marked in red color. The corresponding distances between the N^6 atoms (attachment sites for TEMPO group) are depicted by a green line. The figures were generated from the PDB files using Pymol: parallel-stranded DNA quadruplex structures: 1K8P[3] and 1KF1[3], antiparallel basket type 143D[4], and (3+1) hybrid quadruplex structure 2GKU[5]. *anti* guanines are colored green, *syn* guanines are colored red.

CD Spectroscopy

CD spectra were recorded on a Chirascan CD spectrophotometer (Applied Photophysics) in 10 mM Na_2HPO_4, 150 mM NaCl, pH 7.0, 25°C, with 0.5 nm step size, 2 sec/data point, 3 repetitions. RNA concentration for **5** and **6** was 3 µM, duplex concentration **8**/**7**-**12**/**7** was 1 µM.

[We thank Dr. Dirk Fasshauer, MPI f. Biophysical Chemistry for access to the CD spectrophotometer.]

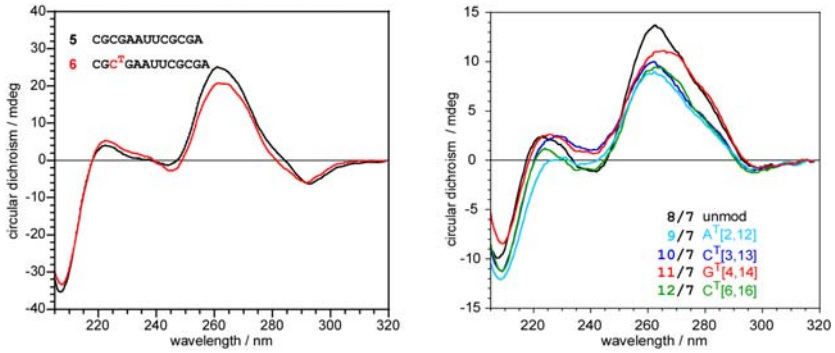

Figure S12. CD of single- and double-TEMPO-labeled RNA duplexes.

Native gel electrophoresis

Gel shift analysis of hairpin and duplex conformations was performed on 15% polyacrylamide gels in 1x TBE buffer at 4°C. Samples were annealed at a concentration of 20 µM RNA in 10 mM K_2HPO_4, 150 mM NaCl, pH 7.0, 90°C 2 min, placed on ice for 2 min, and then mixed with an equal volume of 2x loading buffer (30% glycerol, 1x TBE, 5% bromophenol blue and xylene cyanol dye solution). The samples were loaded at 4°C and the gel was run at 80 V at 4°C. The RNA bands were visualized by staining with ethidium bromide. In a mixture of equal concentrations of RNA **12** and RNA **7**, a minor amount of hairpin conformation was still visible. This is most likely due to a small imprecision in the RNA concentration which was determined by measuring absorbance at 260 nm at room temperature. A slight excess of one or the other strand will result in residual ethidium bromide-stainable material at the position of the hairpin conformation in native gels. (Note: This is in contrast to the PELDOR titration experiment, where the 100% duplex data point results from a mixture that contains excess of unlabeled RNA **7**, and therefore all of RNA **12** will form 100% spin-labeled duplex. The remaining unlabeled RNA **7** in the hairpin conformation is not detectable by EPR).

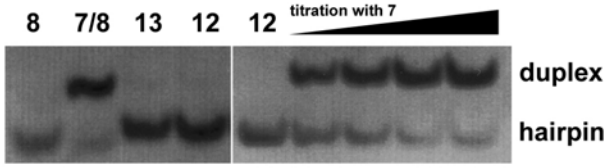

Figure S13. Native gel electrophoresis of hairpin and duplex conformations of TEMPO-labeled and unlabeled RNAs.

References for Supporting Information

[1] G. Jeschke, V. Chechik, P. Ionita, A. Godt, H. Zimmermann, J. Banham, C. R. Timmel, D. Hilger, H. Jung, *Appl. Magn. Reson.* **2006**, *30*, 473.
[2] A.T. Phan, *FEBS J.* **2010**, *227*, 1107.
[3] G.N. Parkinson, M.P.H. Lee, S. Neidle, *Nature* **2002**, *417*, 876.
[4] Y. Wang and D.J. Patel, *Structure* **1993**, *1*, 263.
[5] K.N. Luu, A.T. Phan, V. Kuryavyi, L. Lacroix, D.J. Patel, *J. Am. Chem. Soc.* **2006**, *128*, 9963.